Quantitative Evaluation of Stone Fragments in Extracorporeal Shock Wave Lithotripsy Using a Time Reversal Operator

Jen-Chieh Wang and Yufeng Zhou [a)]

School of Mechanical and Aerospace Engineering, Nanyang Technological University, 50 Nanyang Avenue Singapore 639798

[a)]Corresponding author: YFZHOU@ntu.edu.sg

Abstract. Extracorporeal shock wave lithotripsy (ESWL) has been used widely in the noninvasive treatment of kidney calculi. The fine fragments less than 2 mm in size can be discharged by urination, which determines the success of ESWL. Although ultrasonic and fluorescent imaging are used to localize the calculi, it's challenging to monitor the stone comminution progress, especially at the late stage of ESWL when fragments spread out as a cloud. The lack of real-time and quantitative evaluation makes this procedure semi-blind, resulting in either under- or over-treatment after the legal number of pulses required by FDA. The time reversal operator (TRO) method has the ability to detect point-like scatterers, and the number of non-zero eigenvalues of TRO is equal to that of the scatterers. In this study, the validation of TRO method to identify stones was illustrated from both numerical and experimental results for one to two stones with various sizes and locations. Furthermore, the parameters affecting the performance of TRO method has also been investigated. Overall, TRO method is effective in identifying the fragments in a stone cluster in real-time. Further development of a detection system and evaluation of its performance both *in vitro* and *in vivo* during ESWL is necessary for application.

INTRODUCTION

The extracorporeal shock wave lithotripsy (ESWL) has been a popular method to break kidney stone for thirty years [1, 2]. The main mechanism is using stress and cavitation induced by shock waves to break stones into fine fragments (< 2 mm in diameter) which can be discharged by urination [3]. However, re-sessions and renal injuries (i.e., hematuria, formation of diffuse hemorrhage and multiple hematomas within the renal parenchyma, perirenal fat and subcapsular connective tissue a well as kidney edema) are commonly accompanied with ESWL [4, 5], which may be due to the lack of effective and quantitative monitoring modality for the stone comminution in real time. Currently, X-ray and ultrasonic B-scan imaging are used to diagnose kidney stone and check its fragmentation during ESWL [6, 7]. However, both of them cannot provide sufficient information on the outcome in real time, especially at the late stage of ESWL when fragments spread out as a cloud. Thus the stone patients will undergo the legal number of shock waves required by the US Food and Drug Administration (FDA). This semi-blind procedure may result in either under- (remaining stones for re-sessions) or over-treatment (more renal injury).

Besides the diagnostic methods, acoustic emission and scattering signals were also picked up passively to evaluate the process of ultrasound treatment [8, 9]. Due to the random characteristics of bubble cavitation, the acoustic emission signals in ESWL are unstable. The time reversal operator (TRO) method provides the ability to detect point-like scatterers, and the number of non-zero eigenvalues of TRO is equal to that of the scatterers [10]. The feasibility of applying TRO method to identify stones and the optimal configuration were investigated in this study. Both numerical and experimental results provided the validation of TRO method.

Proceedings from the 14th International Symposium on Therapeutic Ultrasound
AIP Conf. Proc. 1821, 150004-1–150004-5; doi: 10.1063/1.4977648
Published by AIP Publishing. 978-0-7354-1489-1/$30.00

METHODS

The TRO method relies on the transfer matrix, K, between transmitted and received signals as

$$R(\omega) = K(\omega)E(\omega) \tag{1}$$

where ω is the frequency, R and E are the received and transmitted signals, respectively. The number of non-zero eigenvalues of the matrix $K(\omega)^{*}\cdot K(\omega)$ is correlated with the number of scatterers. The discrete expression of the transfer matrix K could be determined in an iterative process:

$$R_n = \sum_{m=1}^{L} K_{nm} E_m \ , \ 1 \le n \le L \tag{2}$$

where L is the number of transmit-receive transducers. If only one pulse, such as a 5-cycle sinusoidal wave, is used, the equation above could be simplified as

$$R_n = K_n E \ , \ 1 \le n \le L' \tag{3}$$

where L' is the number of sensors. Subsequently, the processing time will be decreased significantly.

Both calcium oxalate monohydrate (COM, ρ=2038 kg/m3, c=4535 m/s) and stainless steel (SS, ρ=8000 kg/m3, c=5740 m/s) balls were used in the simulation. A 5-cycle planar low-intensity pulsed ultrasound (LIPUS) burst hits the stone targets from the left and a a sensor array is positioned in a circular with the stone at the center and radius of 45 mm as shown in Fig. 1(a). The acoustic field was simulated using the k-wave method, and matrix operation was run in Matlab (MathWorks, N. Nortick, MA, USA). In addition, experimental results were collected and then compared with the numerical ones. Here, only stainless steel balls were used. The experimental setup is shown in Fig. 1(b). The 5-cycle LIPUS (28.59±0.24 kPa) emitting from a flat transducer (V392, Olympus-IMS, Waltham, MA, USA) was generated by a function generator (AFG 3022B, Tektronix, Beaverton, OR, USA). Scattering signals of stainless steel balls were collected by a hydrophone (PT hydrophone, Institute of Acoustics, Chinese Academy of Sciences, China) and then amplified 50 dB by a pulser/reciver (5072PR, Olympus-IMS, Waltham, MA, USA). A digital oscilloscope (WaveSurfer 44MXs-B, LeCroy, Chestnut Ridge, NY, USA) was synchronized by a DAQ board (USB-6008, National Instruments) triggering function generator to record the waveforms. The hydrophone was moved along a circular stage manually at a step size of 5°.

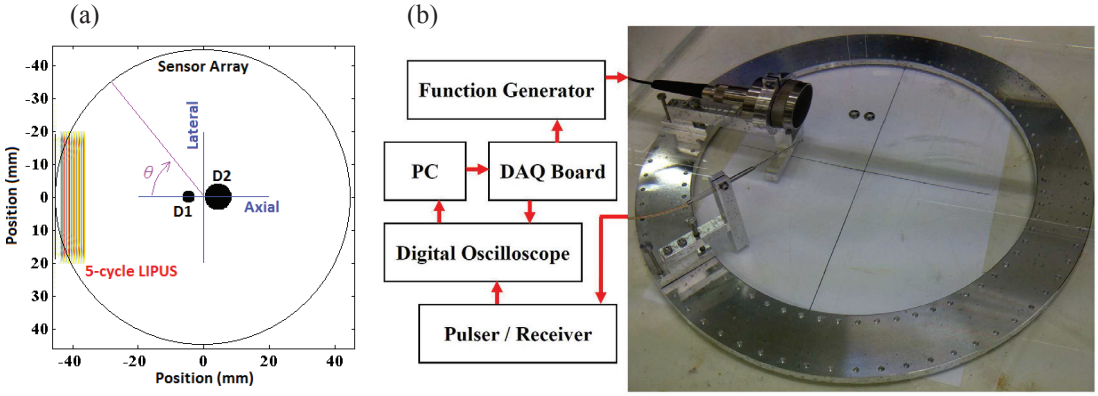

FIGURE 1. Schematic of (a) numerical coordinate and (b) photo of experimental setup.

RESULTS

Eigenvalues were normalized by the first and largest one and higher order ones can be ignored in our study because of the low value (< 10^{-10}). The threshold of 0.146 was set to filter the noise in the experiment, which was determined from the spread distance of statistical results with signal-to-noise ratio (SNR) of 15 dB. In Fig. 2, both numerical (COM and SS) and experimental (SS) results show good agreement on distinguishing the signals of one stone and two axial stones at different frequencies (0.75, 1 and 1.25 MHz). COM and SS balls have no significant difference in the simulation because of their much higher acoustic impedances in comparison to the water. The normalized eigenvalues found in the experiment at the central frequency of LIPUS transducer were close to the

simulated values because of higher excitation efficiency and SNR in the received signals.

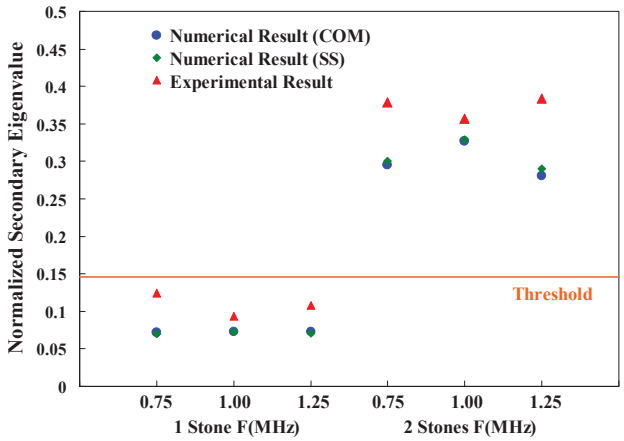

FIGURE 2. Normalized secondary eigenvalues of one stone (diameter = 10 mm) and two axial stones (diameter = 8 mm, gap = 3 mm) with sensor array positioned at 30° ~ 150° and -30° ~ -150°.

Various sensors with different numbers and positions were tested first for the optimal setting. For stone(s) positioned axially symmetric, arrays at the top, bottom, and both sides achieve the same eigenvalues. Results show that sensors covering from 30° to 150° can identify one stone and two axial/lateral stones at the frequency from 0.25 MHz to 2.5 MHz. This set is preferred because it can pick up all scattering fields, but avoid main reflection and diffraction waves (see Fig. 3).

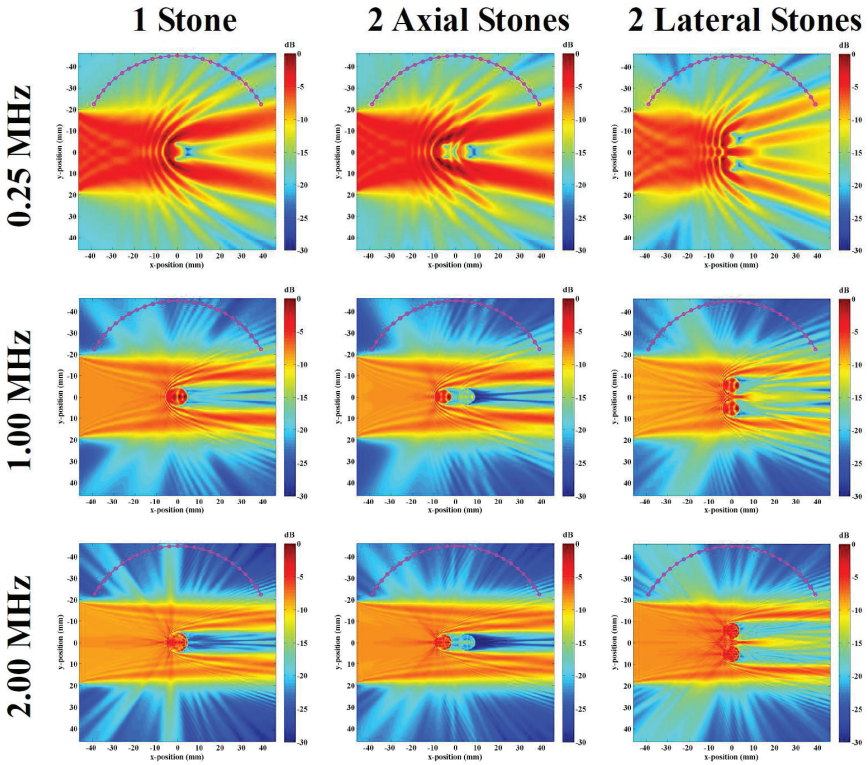

FIGURE 3. Comparison of the scattering fields for various stone settings (one stone with diameter of 10 mm and two axial and lateral stones with diameter of 8 mm and gap of 3 mm) and driving frequency of LIPUS (0.25-2 MHz). Purple dots denote sensor positioned from 30° to 150°.

The resolution of detecting two axial stones increases with the frequency and gap (see Fig. 4a). In contrast,

although the resolution for two lateral stones increases with the frequency, but not the gap (see Fig. 4b). High-frequency waves have less diffraction and more non-divergent beam incident on the stones than low ones, so their detection resolution is high. Both stones located laterally can be exposed by LIPUS without blockage regardless of the gap between them. In contrast, but the rear stone located axially, especially in small size and gap, will generate much less scattering field. Therefore, the key to identify stones is that individual fragment should generate sufficiently large scattering signals for measurement.

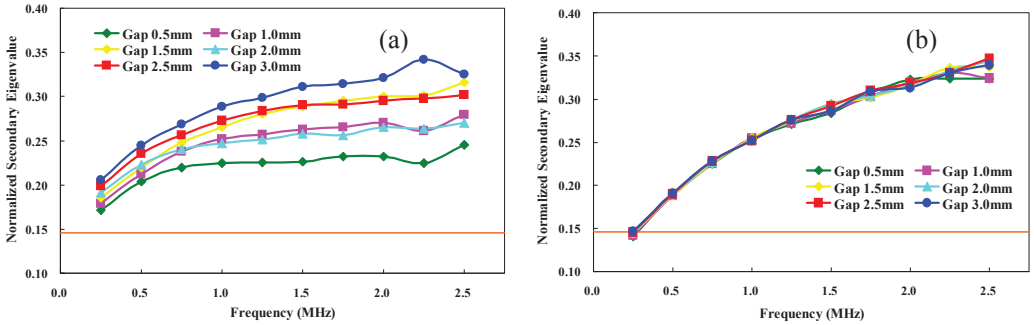

FIGURE 4. Normalized secondary eigenvalues of two (a) axial and (b) lateral stones (diameter = 8 mm) with various gaps.

In addition, two stones with different sizes were also simulated (see Fig. 5a). It shows that if the small stone is blocked and cannot generate the sufficient scattering beams, such as a smaller one aligned behind a large one in the axis, the detection reliability and resolution will become worse (even below the threshold of reliable eigenvalue measurement, 0.146). In contrast, if two stones are aligned laterally, there is no significant difference in the detection resolution and location of the sensor array, either at the same or opposite side of the small one. Fig. 5b shows that two stones with the same size (1-8 mm) can always be identified.

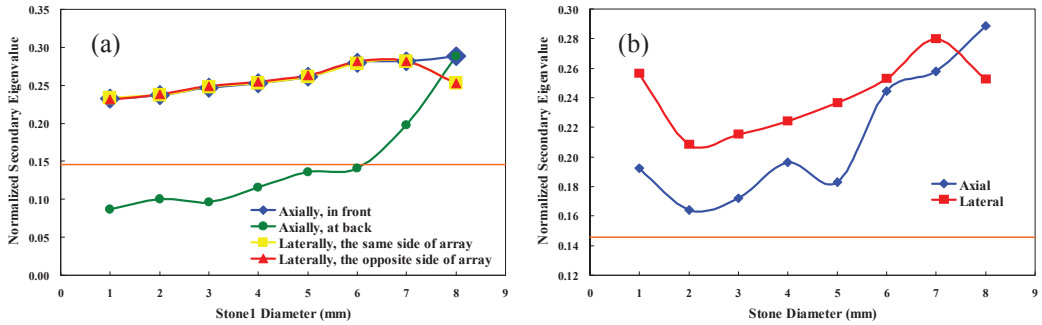

FIGURE 5. Normalized secondary eigenvalues of (a) two stones (D1 = 1~8 mm, D2 = 8 mm) and the smaller one with different location and (b) two stones with the same size along axial and lateral direction.

DISCUSSION

In this study, the TRO method has been evaluated both numerically and experimentally. Results showed a promising capacity of identifying stones. Stones with gap as small as 0.5 mm (Fig. 4a) and diameter as small as 1 mm (Fig. 5b) can be distinguished successfully and reliably. It implies that TRO method may have ability to identify cloudy cluster of fragments which becomes blurred in the current fluoroscopic and ultrasonic images during ESWL and cannot discern the large fragments and evaluate the stone comminution efficiency. However, application of the TRO method to multiple scatters are still under investigation to estimate the size distribution of fragments.

The ordinary targets of the TRO method are point-like scatterers. However, the stone fragments in this study are considered as rigid bodies, which leads to the increased complexity of the scattering field. For example, the scattering field of a spherical rigid ball is the summation of Legendre's and Bessel's function of $cos\theta$ and (ka), respectively, where θ is the scattering angle, k is the wave number and a is the radius of the ball. Theoretically, eigenvalues, λ, of the TRO matrix are

$$\lambda_i = |C_i|^2 (\sum_{j=1}^{L'} |H_{ij}|^2)^2, \; i = 1, 2, \ldots D \tag{4}$$

where C is the reflectivity of each scatterer, H is the wave propagation matrix, and D is the number of scatterers. It implies that identical scatterers should have the same eigenvalues. However, two stones with the same diameter positioned laterally, which yields a spatial symmetry, still have difference between the first and second eigenvalues (see Fig. 5b). The reason may be the inacurrate description of the wave propagation matrix in the TRO algorithm. In order to solve it, the multiple signal classification (MUSIC) algorithm [11], which has more specifics of spatial propagation, will be tried in the near future.

Focused shock wave could be used as the sound source for the generation of scattering waves from stone fragments. However, the analysis of echo signals is more complicated. Although the acoustic emission due to bubble collapse can be filtered out in the time domain (>100 μ s), the quick collapse of small bubbles (<20 μ s) around stone surface by the compressive component of lithotripter shock wave and the scattering of existing bubbles along the path of wave propagation will also serve as emission sources.

CONCLUSIONS

Only one non-zero eigenvalue for a single stone showed the stability of TRO method. Our algorithm can also figure out the presence of two stones in different sizes and locations. Various sets of sensor array, the positions of the stones, and frequencies of incident waves were tested for the optimal configuration. Frequency of incident wave determines the scattering field, and subsequent detection outcome. High frequency provides better resolution. The location of the sensor array is important in reliable and accurate stone detection, and the best location of sensor array was found to be $30^\circ \sim 150^\circ$, which can measure most scattering field, but avoid the main wave reflection and diffraction. As long as the stone fragment can generate the sufficiently strong scattering, it can be detected. Otherwise, the TRO method has poor performance Because of the short computation time, the TRO method has good capacity of real-time application during ESWL treatment.

REFERENCES

1. C. Chaussy, W. Brendel and E. Schmiedt, Lancet **2** (8207), 1265-1268 (1980).
2. C. Chaussy, E. Schmiedt, D. Jocham, W. Brendel, B. Forssmann and V. Walther, J Urol **127** (3), 417-420 (1982).
3. S. Zhu, F. H. Cocks, G. M. Preminger and P. Zhong, Ultrasound Med Biol **28** (5), 661-671 (2002).
4. Y. M. Tan, S. K. Yip, T. W. Chong, M. Y. Wong, C. Cheng and K. T. Foo, Scand J Urol Nephrol **36** (5), 363-367 (2002).
5. J. A. McAteer, A. P. Evan, L. R. Willis, B. A. Connors, J. C. Williams, Y. A. Pishchalnikov and J. E. Lingeman, Aip Conf Proc **900**, 287-301 (2007).
6. G. Heine, Z Urol Nephrol **73** (3), 223-228 (1980).
7. A. Pytel' Iu, V. N. Demidov, G. Aliaev Iu, V. A. Chabanov and A. V. Amosov, Urol Nefrol (Mosk) (6), 8-12 (1981).
8. N. R. Owen, M. R. Bailey, L. A. Crum, O. A. Sapozhnikov and L. A. Trusov, J Acoust Soc Am **121** (1), EL41-47 (2007).
9. T. G. Leighton, F. Fedele, A. J. Coleman, C. McCarthy, S. Ryves, A. M. Hurrell, A. De Stefano and P. R. White, Ultrasound Med Biol **34** (10), 1651-1665 (2008).
10. C. Prada, S. Manneville, D. Spoliansky and M. Fink, Journal of the Acoustical Society of America **99** (4), 2067-2076 (1996).
11. R. O. Schmidt, Ieee T Antenn Propag **34** (3), 276-280 (1986).